

# Lateral Diffusion in Substrate-Supported Lipid Monolayers as a Function of Ambient Relative Humidity

Tobias Baumgart and Andreas Offenhäusser

Max-Planck Institute for Polymer Research, D-55128 Mainz, Germany

**ABSTRACT** We analyzed the influence of water activity on the lateral self-diffusion of supported phospholipid monolayers. Lipid monolayer membranes were supported by polysaccharide cushions (chitosan and agarose), or glass. A simple diffusion model was derived, based on activated diffusion with an activation energy,  $E_a$ , which depends on the hydration state of the lipid headgroup. A crucial assumption of the derived model is that  $E_a$  can be calculated assuming an exponential decay of the humidity-dependent disjoining pressure in the monolayer/substrate interface with respect to the equilibrium separation distance. A plot of  $\ln(D)$  against  $\ln(p_0/p)$ , where  $D$  is the measured diffusion coefficient and  $p_0$  and  $p$  are the partial water pressures at saturation and at a particular relative humidity, respectively, was observed to be linear in all cases (i.e., for differing lipids, lateral monolayer pressures, temperatures, and substrates), in accordance with the above-mentioned diffusion model. No indications for humidity-induced first-order phase transitions in the supported phospholipid monolayers were found. Many biological processes such as vesicle fusion and recognition processes involve dehydration/hydration cycles, and it can be expected that the water activity significantly affects the kinetics of these processes in a manner similar to that examined in the present work.

## INTRODUCTION

Lipid membranes supported by a planar substrate receive considerable interest both from basic research and due to their applications in terms of biosensing (Sackmann, 1996; Sackmann and Tanaka, 2000). The fluidity of the membrane in terms of lateral self-diffusion is considered to be an important, if not essential, condition of biomimetic lipid membranes. While vast literature exists concerning diffusion of lipid molecules in free and supported model and biological *bilayer*-membranes (Clegg and Vaz, 1985; Almeida and Vaz, 1995), and in monolayers at the air/water interface (e.g., Peters and Beck, 1983), experimental data concerning the fluidity of *supported monolayers* of amphiphiles in general, and phospholipids in particular, are relatively scarce.

The lateral diffusion of fully hydrated monolayers on hydrophobic supports was measured in Merkel et al., 1989, using the technique of fluorescence recovery after photobleaching (FRAP). In other studies hydrogels were used as a hydrophilic support for phospholipid monolayers and were found to enhance monolayer fluidity compared to glass supports in a water-saturated atmosphere (Kühner et al., 1994; Dietrich and Tampe, 1995). Furthermore, polyelectrolytes were coated with a planar lipid monolayer and the fluidity was determined by a fringe pattern photobleaching technique after immersing the substrate in different solvents and in air (Auch et al., 2000).

Several authors point to the influence of humidity on the dynamics of supported amphiphile monolayers (Chen et al., 1989; Chi et al., 1992a; Chen and Israelachvili, 1992; Berman et al., 1997; Shiku and Dunn, 1998). During the exposure of a supported lipid monolayer to a high-humidity atmosphere, water permeates the hydrophobic part (Vanderveen and Barnes, 1985) and the headgroups become hydrated, as observed for example, by a thickness increase of the monolayer (Chen and Israelachvili, 1992; Bolze J. et al., 2002) accompanied by a weakening of the monolayer substrate interaction (Yaminsky et al., 1997). A systematic study of the effects of humidity changes on supported monolayer dynamics, however, to the best of the authors' knowledge, is missing completely.

This is not the case for bilayers: McCown et al. (1981) analyzed the influence of humidity changes on the lateral diffusion of membrane probes added to a multibilayer stack. The decrease of fluidity at lower humidities (even though the acyl chains remained in the fluid state) was assumed to be due to 1) the smaller area per lipid headgroup, and 2) the smaller volume fraction of the polar headgroup in the aqueous region. The latter influences lipid mobility due to the proximity of the opposing headgroup. Galle and Volke developed a model that includes influences of temperature and humidity based on the Arrhenius expression for activated diffusion (Galle and Volke, 1995). Again, the influence of humidity was assumed to be due to its influence on the lipid headgroup area, hence on the free area available for diffusion (see below). The mobility of surfactant monolayers deposited onto silica surfaces was analyzed in Neuman et al. (1994); however, the authors used a rather special setup, resembling a surface force apparatus, and performed bleaching experiments in the contact zone of two monolayer-coated surfaces only. The aim of the present work is to characterize the lipid-membrane/substrate interface with re-

---

Submitted November 20, 2001, and accepted for publication May 8, 2002.

Address reprint requests to Andreas Offenhäusser, Institute for Thin Films and Interfaces, Forschungszentrum Jülich, D-52425 Jülich, Germany. Tel.: +49-2461-61-2330; Fax: +49-2461-61-2333; E-mail: a.offenhaeuser@fz-juelich.de.

© 2002 by the Biophysical Society

0006-3495/02/09/1489/12 \$2.00

spect to its influence on membrane mobility. Supported lipid monolayers are particularly well suited for this purpose due to their robustness and insensitivity toward substrate inhomogeneities compared to supported bilayers (Kühner et al., 1994), and the fact that the disjoining pressure in the membrane/substrate interface may be changed readily over a wide range by adjusting the ambient humidity. In the present work, lipid monolayer membranes were either supported by thin polymer cushions or by a glass substrate.

## MATERIALS AND METHODS

### Lipids

The phospholipids DMPC (1,2-dimyristoyl-*sn*-glycero-3-phosphatidylcholine) and DPhyPC (1,2-diphytanoyl-*sn*-glycero-3-phosphatidylcholine) were purchased from Avanti Polar Lipids (Alabaster, AL), and used without purification. The following fluorescence membrane probes were used for staining the lipid monolayers: *N*-(7-nitrobenz-2-oxa-1,3-diazol-4-yl)-1,2-dihexadecanoyl-*sn*-glycero-3-phosphoethanolamine, triethylammonium salt (NBD-PE), 22-(*N*-(7-nitrobenz-2-oxa-1,3-diazol-4-yl)amino)-23,24-bisnor-5-cholesterol (NBD-Chol), Molecular Probes (Leiden, the Netherlands), and 1-myristoyl-2-[12-[(7-nitro-2-1,3-benzoxadiazol-4-yl)amino]dodecanoyl]-*sn*-glycero-3-phosphocholine (NBD-PC), Avanti Polar Lipids. The fluorescence probes were added to the lipid solution at a concentration of 1 mol % with respect to the host lipid.

### Polymer cushions

Chitosan and agarose were obtained from Sigma-Aldrich (Seelze, Germany), and used without purification. Chitosan was dissolved in a 1% v/v acetic acid solution (99.8%, Riedel-de Haën, Seelze, Germany) (Blair et al., 1987) at a concentration of 1% w/w by stirring overnight. The solutions were filtered through syringe filters (Millex, Millipore, Corp., Bedford, MA) with a pore size of 5  $\mu\text{m}$ . Afterward the solutions were centrifuged (Biofuge 22R, Heraeus, Osterode, Germany) for 30 min at a speed of 11,400 rpm. Thin chitosan films were prepared by spin-coating the chitosan solution onto cleaned, hydrophilic glass slides (Mettler Glas, Rettberg, Göttingen, Germany, length 3.2 cm, width 2.6 cm, thickness 150–180  $\mu\text{m}$ ). Substrate cleaning was performed by sonication in a 2% v/v Hellmanex solution (Hellma, Müllheim, Germany), followed by thoroughly rinsing the substrates in Millipore water. Spin-coating was typically performed at a spinning speed of 3000 rpm, which yielded film thicknesses around 140 nm as determined by ellipsometry. To neutralize the films, the polymer-covered substrates were immersed for several hours in a borate buffer (pH 9.22, Merck, Darmstadt, Germany) and afterward rinsed in Millipore filtered water. Agarose films were prepared by dipping clean substrates into a hot agarose solution of a concentration of 0.2% w/w. Upon quickly withdrawing, a thin polymer film remained on the glass and formed a thin gel film upon cooling (Dietrich and Tampe, 1995).

### FRAP

For determining lateral self-diffusion coefficients, the method of fluorescence recovery after photobleaching (FRAP) of membrane labels was used (Axelrod et al., 1976; Györfvay et al., 1999). By means of intense laser light a spot of a diameter of  $\sim 4 \mu\text{m}$  was bleached. The exchange of bleached and unbleached molecules due to lateral diffusion leads to a recovery of the initial fluorescence intensity, which was observed by means of low-intensity laser light and a photomultiplier.

The central part of the FRAP apparatus was an inverted microscope (IX-70, Olympus, Hamburg, Germany). A mercury burner (HBO 100,

Olympus) allowed for illumination of the whole observation field. For fluorescence microscopy, a fluorescence cube consisting of an excitation bandpass filter (BP 470–490, Olympus) and a barrier filter (BA 515, fluorescence cube U-MNIB, Olympus) was used. FRAP experiments were performed with an argon ion laser (Innova 90/4, Coherent, Dieburg, Germany), which was operated at a wavelength of 488 nm (at a power of 1.2 W). A combination of three pockels cells and four linear polarizers (Gsänger, München, Germany) in an alternating arrangement permitted beam attenuation by a factor of  $10^{-6}$ . Changing the pockels cell voltage provided adjustment of the observation intensity, which is necessary to avoid photobleaching during intensity measurements.

Bleaching was performed by a high-voltage switch (Solatron, Warsaw, Poland), with switching times smaller than 60  $\mu\text{s}$ . The bleaching time was adjustable and was usually set to 40 ms. This bleach interval is a compromise between a time long enough for strong bleaching and a time short enough not to allow significant diffusion during bleaching. The measurement of the fluorescence intensity was performed by means of a photomultiplier tube (9893/100, Thorn EMI, Middlesex, UK). During bleaching, the photomultiplier was gated. Gating, high-voltage switching, photomultiplier counting, and shutter control (see below) were performed with the help of a real time card (ADwin 41d, Jäger, Lorsch, Germany) which allowed for the communication between PC and measurement hardware by means of the software ADbasic (Jäger). The software Testpoint (Keithley Instruments, Germering, Germany) provided a user interface for device control and data representation. Focus adjustment (and fluorescence microscopy) could be performed by means of a light-enhancing camera (extended ISIS, Photonic Sciences, East Sussex, UK).

Because in the present work small diffusion coefficients of partially dehydrated lipid membranes were measured, care had to be taken to avoid bleaching through the observation beam, i.e., before exertion of the bleach pulse or after bleaching. Accordingly, a computer-controlled mechanical shutter (Uniblitz D122, Vincent Associates, Rochester, NY) was inserted into the illumination pathway, which allowed for illumination of the sample during defined observation intervals only. As the switching of the mechanical shutter was too slow in case of fast diffusion, the shutter mechanism was activated at a relative humidity (*RH*) around 80%. The observation interval density was chosen to increase exponentially with smaller observation time.

FRAP experiments were performed under controlled humidity, as described below. The microscope objective was optically coupled to the substrate by means of immersion oil and the setup was allowed to equilibrate at *RH* = 50% for at least half an hour before starting with the first measurement. The relative humidity was then increased to *RH* = 90%. At least five bleaching experiments were performed on different locations of the sample to allow for appropriate error estimation and averaging. As reversibility was found, all measurement series were begun at *RH* = 90% and the relative humidity was then decreased in steps of  $\Delta RH = 2.5\%$ . After performing an alteration of *RH*, the sample was allowed to equilibrate for 5 min before starting a new set of diffusion measurements. If not indicated otherwise, all diffusion experiments were performed at 26°C, which was equal to the ambient temperature. Data evaluation of FRAP experiments was performed as described in Györfvay et al. (1999).

### Humidity adjustment

The relative humidity inside the measurement chamber (see Fig. 1) was adjusted by the mixing of a dry and a water-saturated gas stream (Wolff, 1998). The water-rich gas was produced by bubbling nitrogen through a series connection of two water-filled bottles, the dry gas was obtained by passing a nitrogen gas stream through a series connection of two silica gel-filled bottles. Computer-controlled valves (type 1259C-10000SV, MKS Instruments, Andover, MA) allowed for changing the mixing ratios at a constant total flow. Mixing of the two gas streams occurred shortly before the gas entered the measurement chamber, to decrease the response time of the humidity sensor toward changes of the mixing ratio. Care was

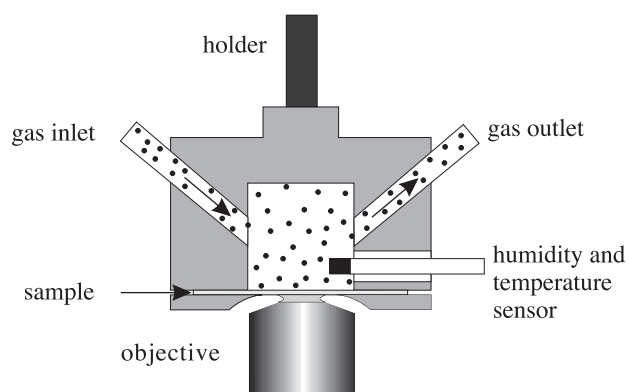


FIGURE 1 Humidity chamber for FRAP measurements and microscopic observation on supported lipid monolayers. The chamber walls were temperature-controlled by a water circle. The temperature and humidity sensor was thermally isolated from the chamber walls by a Teflon capsule. Before optically coupling the oil immersion objective to the sample back side (microscopic coverglass), lipid on the back side of the coverglass was thoroughly wiped off with isopropanol.

taken to avoid water droplets from creeping along the gas tubes and entering the measurement chamber. Therefore, a water trap was inserted into the wet gas tube and the final part of the mixed gas tube was filled with cotton wool. *RH* was determined by measuring both temperature and gas phase water content in the measurement chamber. The humidity and temperature sensor was a Hygroclip miniature air probe with A1H interface, Rotronic, Ettingen, Germany. The transducer was equipped with an RS 232 interface, which enabled data readout by a PC. A feedback loop allowed for adjusting *RH* to the desired value.

### Solvent gas variations

Monolayers were exposed to different solvent gases (dimethyl sulfoxide (DMSO), isopropanol, chloroform, ethanol, obtained from Sigma-Aldrich), by placing a small, open container filled with the particular solvent into the sealed measurement chamber. The atmosphere was allowed to equilibrate for 1 h and it was ensured that no condensation of solvent droplets on the sample surface occurred.

### Langmuir-Blodgett transfer

For the preparation of Langmuir-Blodgett monolayers a trough with a mechanical dipper and Wilhelmy balance was used (NIMA Technology Ltd., Coventry, UK). The subphase consisted of ion exchanged Millipore filtered water (Millipore Milli-Q system,  $R = 18.2 \text{ M}\Omega \text{ cm}$ ). Monolayers were obtained by spreading a lipid solution (chloroform, 1 mg/ml) on the trough subphase. After spreading the lipid solution the solvent was allowed to evaporate (for half an hour) and the film was compressed to the desired lateral pressure ( $T = 25^\circ\text{C}$ ). After completion of compression, the film was allowed to equilibrate for half an hour and finally deposited at a speed of 4 mm/min. Before mounting the monolayer covered glass substrates into the humidity chamber, lipid transferred to the back side of the substrate was thoroughly wiped off with an isopropanol-soaked tissue.

## RESULTS

Lateral self-diffusion coefficients of lipid probes in phospholipid membranes supported by polymer cushions were

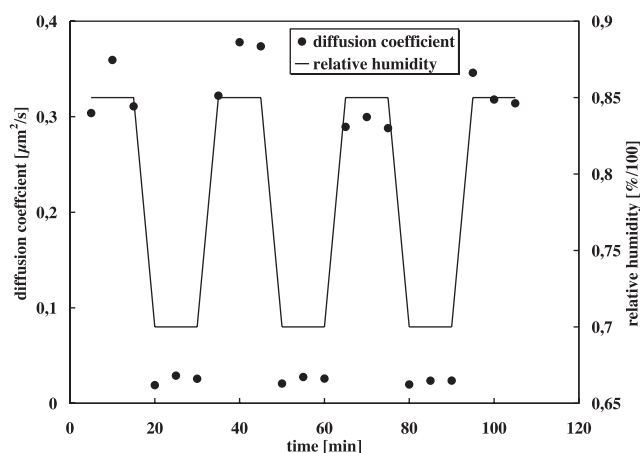


FIGURE 2 Reversibility of changes of the diffusion coefficient (dots) upon switching between different ambient humidities (line), in a DMPC monolayer on chitosan, lateral pressure 35 mN/m, fluorescence probe NBD-PE.

found to be highly dependent on ambient humidity. However, complete reversibility was found while changing *RH* between 70% and 85% (Fig. 2). Furthermore, pronounced drying at  $RH \approx 4\%$ , which was the lower limit of the humidity setup, did not lead to irreversible changes of diffusion coefficients (data not shown). From the reversibility of the monolayer fluidity, it can thus be concluded that harsh changes in *RH* did not lead to irreversible morphological distortions in the monolayer or at the polymer surface. Moreover, while diffusion coefficients were depending on *RH*, the relative recovery, *R*, was in all cases of the experiments described in the following close to or equal to one. This indicates a complete fluorescence recovery in the whole accessible humidity range.

Prolonged annealing times at high humidities revealed that the monolayer fluidity did not increase after further annealing. Therefore, after reaching a certain humidity, which took seconds to minutes depending on the direction and steepness of the jump, no further swelling at the monolayer/polymer interface occurred.

### Lateral self-diffusion in phosphatidylcholine monolayers in different hydration states

Detailed studies concerning the influence of humidity on lipid self-diffusion in monolayers were carried out in a humidity range of 90% down to 65% to 50%, depending on the mobility found for low hydration states. The upper value was chosen because the error in determining *RH* largely depends on the magnitude of the relative humidity; at high humidities small temperature gradients can produce large differences in *RH*. At the lower boundary the resolution limit of the FRAP setup was encountered, which is determined by laser stability, mechanical stability of the setup, and probe stability. The lower boundary for the diffusion

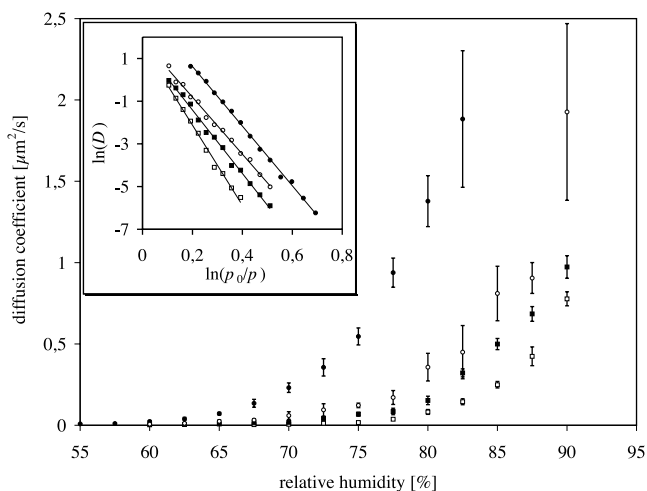


FIGURE 3 Diffusion coefficients of a chitosan-cushioned lipid monolayer, lateral pressure 35 mN/m. The inset shows an axis transformation of the same data sets, the natural logarithm of  $D$  is plotted against the natural logarithm of  $p_0/p = 100/RH$ . ○ Lipid: DMPC, fluorescence probe: NBD-PE, temperature 26°C, slope:  $-13.36$ , intercept 1.86. ● Lipid: DMPC, fluorescence probe: NBD-PC, temperature 30°C, slope:  $-13.97$ , intercept 3.42. ■ Lipid: DMPC, fluorescence probe: NBD-Chol, temperature 26°C, slope:  $-14.87$ , intercept 1.56. □ Lipid: DPhyPC, fluorescence probe: NBD-PE, temperature 26°C, slope:  $-18.78$ , intercept 1.63.

coefficient in the case of the present setup was found to be around a value of  $10^{-3} \mu\text{m}^2/\text{s}$ . In the range of this value, data scattering became too high and recovery times became too long to be reasonable from a practical point of view.

Fig. 3 shows the reduction of the diffusion coefficient with decreasing  $RH$  in a DMPC layer that was stained with the headgroup-labeled membrane probe NBD-PE and transferred at a lateral pressure of 35 mN/m (the influence of labeling at the headgroup on the reporter ability of the probe will be analyzed below).

Fig. 3 shows the reduction of the diffusion coefficient with decreasing  $RH$  in monolayers stained with different fluorescence dyes and composed of different lipids. All the measurements presented in Fig. 3 were obtained with monolayers that were transferred at a lateral pressure of 35 mN/m. In all cases, an axis transformation in terms of a double logarithmic plot of the diffusion coefficient against the ratio of the partial water pressures,  $p_0/p$ , leads to an essentially straight line (see the inset in Fig. 3). The partial pressure  $p_0$  refers to water saturation, and  $p$  is the value at the humidity  $RH = 100 p/p_0$ . The linear relationship in the axis-transformed plot was found in all measurements described in the present work. The following discussion will therefore refer to the linearized plots. The rationale behind this data representation will be provided in the Discussion.

To test for a possible influence of the fluorescence label on the humidity dependence of diffusion coefficients besides NBD-PE, the tail-labeled phospholipid NBD-PC was used (Fig. 3). Within the experimental error, the same slope

(within the axis-transformed plot) as in the case of NBD-PE labels was found. Due to a slightly higher temperature (30°C compared to 26°C in the case of NBD-PE) the intercept is higher as compared to monolayers labeled with NBD-PE. It is known that the fluorescence label NBD in the case of NBD-PC stained, completely hydrated lipid bilayers is located in the polar region of the membrane, although the fluorescence probe is attached to the unpolar tail of the lipid molecule (Chattopadhyay, 1990). This, however, must not necessarily refer to a partially dehydrated solid-supported monolayer also. However, to further prove that a disturbing effect of the fluorescence probe can be neglected in the present kind of experiment, an NBD-labeled cholesterol derivative (NBD-Chol) was used. The label of the latter is known to be located in the nonpolar region of completely hydrated lipid bilayers (Chattopadhyay and Mukherjee, 1999). As shown in Fig. 3, the measured slope (at a temperature of 26°C) is in accordance (within the experimental accuracy) with the values found for NBD-PE-labeled DMPC monolayers, whereas the intercept in the latter case is slightly higher.

The similarity between the data sets obtained for the three different membrane labels clearly indicates that all the three probes essentially monitor the lateral fluidity of the host matrix. It is known for hydrophobic probe molecules that independently of their size, the lateral fluidity of the lipid matrix is probed (Balcom and Petersen, 1993), hence the values found for NBD-Chol are comparable to those obtained using NBD-PE.

In multibilayer stacks the reduction of  $RH$  exerts an effective lateral pressure, which compresses the membrane and induces phase transitions (Sirota et al., 1988). However, in the monolayer studies carried out in the present work, no discontinuities, which would indicate first-order phase transitions, were found in the examined data range. To elucidate a possible contribution of humidity-induced phase changes on the lateral fluidity, monolayers of DPhyPC were prepared, that were stained with NBD-PE. The lipid DPhyPC does not show phase transitions in bilayers down to a temperature of  $-120^\circ\text{C}$  (Lindsey et al., 1979). As by dehydration the same transitions can be induced by temperature reduction, DPhyPC is assumed to remain in the liquid-expanded state upon dehydration.

Apart from a slightly higher slope compared to DMPC monolayers subject to corresponding conditions, the same relation between lateral diffusion and relative humidity was found (Fig. 3). The hypothesis of the absence of a lateral compression of the lipid membrane induced by dehydrating the lipid heads is also strongly supported by the fact that a variation of the monolayer density (adjusted on the LB-trough) did not lead to significant changes in the observed behavior (linearity throughout the examined humidity range (Fig. 4).

At high hydration levels the fluidity increased with decreasing lateral pressure (compare the intercepts of the



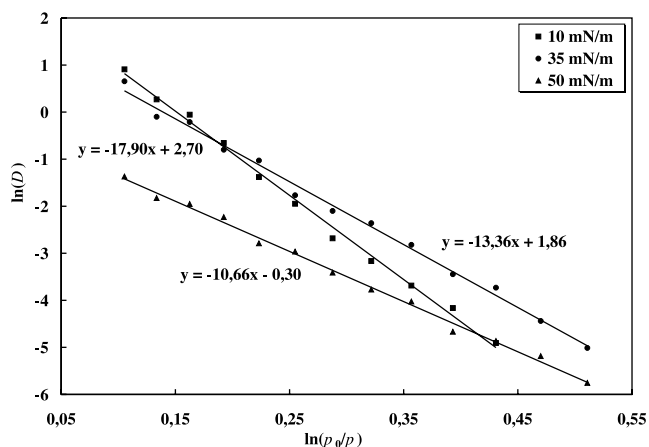


FIGURE 4 Double logarithmic plots of diffusion constants measured in DMPC monolayers on chitosan, transferred at the lateral pressures of 10, 35, and 50 mN/m, fluorescence probe NBD-PE, temperature 26°C.

linear fits in Fig. 4. This is readily explained by the free area theory (Eq. 4): the higher the lateral pressure, the lower is the average free area available for diffusion, hence the diffusion coefficient drops (Galla et al., 1979). Additionally, with a higher lateral pressure, the slopes of the linear fits decreased.

#### Variation of the substrate: agarose and glass

To examine the influence of the lipid membrane support on the humidity dependence of the membrane fluidity, a DMPC monolayer was transferred onto a thin agarose cushion and analyzed in terms of lateral diffusion with respect to changes in *RH* (Fig. 5). A linear relationship in the usual axis-transformed plot was found, as in all experiments per-

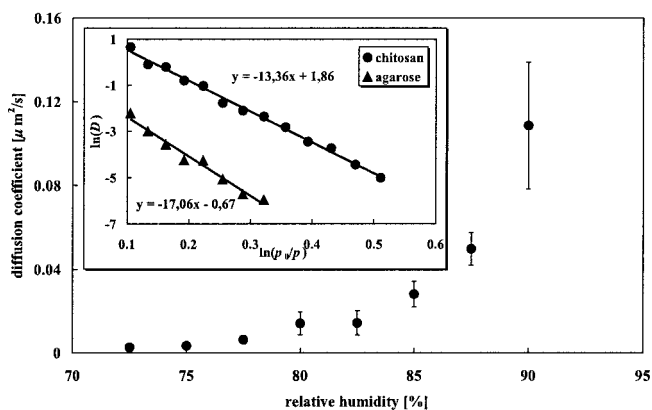


FIGURE 5 Diffusion coefficients in an agarose-cushioned DMPC monolayer, lateral pressure 35 mN/m, fluorescence probe: NBD-PE, temperature 26°C. The inset shows an axis transformation of the same data set. Additionally, for comparison the data for a chitosan-supported monolayer prepared and analyzed under the same conditions was added to the diagram shown in the inset.

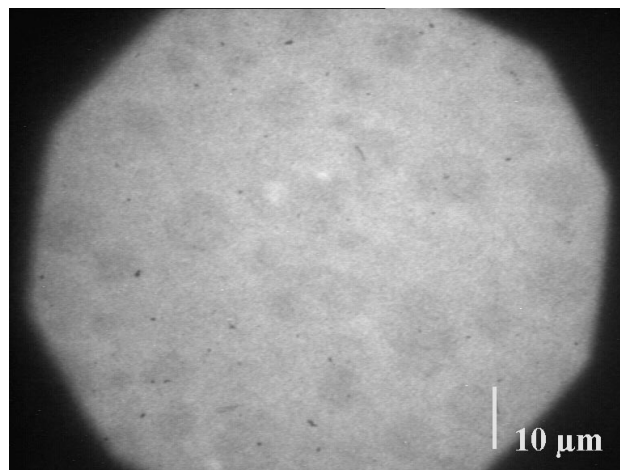


FIGURE 6 Fluorescence image of a DMPC monolayer (lateral pressure 35 mN/m, fluorescence probe NBD-PC, temperature 26°C) on a glass surface; the lipid tails were facing towards a MilliQ-water bulk face.

formed on chitosan cushions. Agarose possesses totally different molecular and packing properties compared to chitosan. The generally reduced fluidity in case of agarose-cushioned DMPC monolayers may be due to either a substrate-mediated condensation or the much higher surface roughness of agarose compared to chitosan (Baumgart, 2001). To clarify this matter, temperature variations would have to be carried out.

In another set of experiments, polymer cushions were omitted completely and the lipid monolayer was transferred directly to the glass surface. The diffusion coefficients were remarkably lower as compared to water-swallowable polymer supports. At a relative humidity of 90%, in a DMPC matrix with the lateral pressure of 35 mN/m, using the fluorescence probe NBD-PC, a value of  $D = 4.9 \cdot 10^{-3} \mu\text{m}^2/\text{s}$  was found (at room temperature). As this value is already rather close to the resolution limit of the FRAP setup, no systematic analysis of the response toward humidity changes could be carried out. However, it was shown that by a further increase of relative humidity to 100% (by pouring MilliQ water on top of the monolayer), the lateral self-diffusion could be increased remarkably. As can be seen in Fig. 6, the monolayer was rather stable and had an almost totally homogeneous appearance, even though the hydrophobic tails of the lipid molecule were exposed directly to water.

The stability of supported lipid monolayers immersed in a series of different liquids has been shown previously (Auch et al., 2000). In the case of a glass-supported lipid monolayer immersed in water we obtained a diffusion coefficient of  $D = 0.17 \pm 0.008 \mu\text{m}^2/\text{s}$ , which is almost two orders of magnitude higher, compared to the value found at  $RH = 90\%$ . To examine the influence of *RH* on lateral diffusion in glass-supported monolayers more systematically, therefore, the humidity range of 90% to 100% would

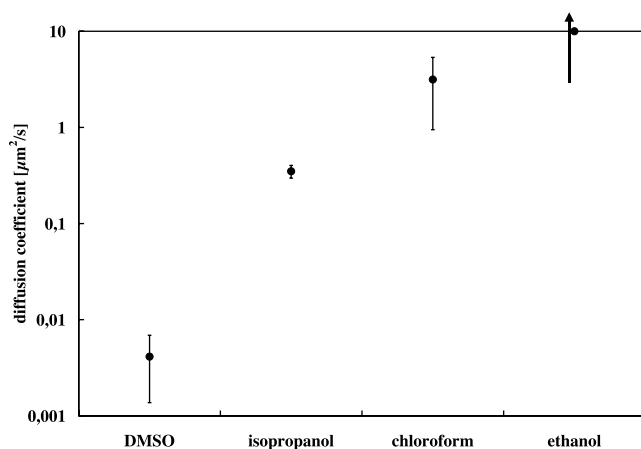


FIGURE 7 Diffusion coefficients of DMPC monolayers, lateral pressure 35 mN/m, supported by a chitosan film. The monolayer was exposed to the indicated saturated atmospheres. The diffusion coefficient for ethanol was found to be too high for being resolvable by the FRAP setup, as indicated by the arrow.

have to be explored. This, however, would necessitate a considerably more precise temperature and *RH* control, which would be possible by a much refined experimental setup only, which in the present work could not be performed.

### Influence of nonaqueous solvents present in the surrounding gas phase

Finally, it was examined qualitatively, in as far nonaqueous gaseous solvents (DMSO, isopropanol, chloroform, ethanol) influence diffusion properties of solid-supported monolayers. It has been found for several nonaqueous solvents that osmotic pressure/distance curves show essentially an exponential dependence (Eq. 8), as in the case of water (McIntosh et al., 1989). While a systematic variation of partial pressures of nonaqueous solvents could not be carried out in the present work, it could be shown qualitatively that their presence in the gas phase could substantially elevate diffusion coefficients of monolayers (Fig. 7). In the case of ethanol, diffusion was so fast that diffusion coefficients could not be determined, as indicated by the arrow in Fig. 7.

Ethanol is known to bind to the lipid-water interface and to modify both headgroup and hydrophobic chain conformations (see Ho and Stubbs, 1997, and references therein). Similar interactions can be assumed to occur in other solvents. The dependence of diffusion constants in DMPC monolayers on solvents present in the surrounding gas phase is not only influenced by lipid/solvent interactions, but also includes the vapor pressures of the solvents. Due to the difficulty of controlling the partial pressures of the latter, systematic studies were not performed.

## DISCUSSION

The water activity  $a_w = p/p_0$  in the gas phase above a hydrogel-supported lipid monolayer was shown to have a remarkable, reversible influence on the magnitude of self-diffusion coefficients of a supported lipid matrix. This dependence shall be examined in the following. Generally, two different approaches for modeling diffusion in amphiphile membranes can be distinguished: hydrodynamic models based on continuum mechanics, and microscopic models, which take into account the discreteness of the lipid matrix (Clegg and Vaz, 1985).

Concerning the former, hydrodynamic equations are used to calculate the friction coefficient  $f$ , which is related to the two-dimensional diffusion coefficient  $D$  by the well-known Einstein relation (Almeida and Vaz, 1995):

$$D = kT/f \quad (1)$$

where  $k$  is Boltzmann's constant and  $T$  is the temperature. Evans and Sackmann (1988) examined the effect of weak dynamic coupling of a membrane to an adjacent support and found

$$f = 4\pi\eta h \left( \frac{\varepsilon^2}{4} + \frac{\varepsilon I_1(\varepsilon)}{I_0(\varepsilon)} \right)^{-1} \quad (2)$$

where  $I_0$  and  $I_1$  are modified Bessel functions of the second kind, orders zero and one,  $\eta$  is the membrane viscosity,  $h$  is the membrane thickness, and

$$\varepsilon = R \left( \frac{b_s}{\eta h} \right)^{0.5} \quad (3)$$

where  $b_s$  is a friction coefficient.

The friction coefficient,  $b_s$ , of a membrane floating on an ultrathin water film, can be calculated by assuming a linear velocity gradient in the water film:  $b_s = \eta_w/d$ , where  $d$  is the thickness of the water film, and  $\eta_w$  is the water viscosity.

According to Eq. 2, to calculate the friction coefficient,  $b_s$ , the parameters  $\eta$ ,  $h$ , and  $R$  have to be determined. The membrane thickness,  $h$ , and radius of the lipid probe,  $R$ , are known from the literature (Merkel et al., 1989). The membrane viscosity,  $\eta$ , can be calculated from diffusion measurements in freely suspended bilayers or in monolayers at the air/water interface, by means of the Saffmann-Delbrück equation (Saffmann, 1975). Using a typical monolayer surface viscosity (Merkel et al., 1989) the dependency of the measured diffusion coefficient on  $b_s$  can be calculated according to Eq. 2. The membrane viscosity is supposed to be independent of *RH*. This assumption is justified by the fact that no indications for humidity-induced lateral compression of the monolayer were found. Assuming, furthermore, a linear velocity gradient in a thin lubricating water film between monolayer membrane and polymer cushion and a no-slip boundary at the surface of the polymer cushion, it turned out that the reduction of the diffusion coefficient was

much too high to be describable by dissipation in a thinning water layer. With the relation  $d = \eta_w/b_s$  a hypothetical lubrication layer thickness was calculated, which was much below the thickness of a monomolecular water layer (Baumgart, 2001). Therefore, the assumption of a continuous water layer between lipid monolayer and underlying substrate is not justified in the present case.

Although the Evans-Sackmann model was used for determining frictional coefficients of lipid probes (Merkel et al., 1989), according to Almeida and Vaz (1995) it is questionable if the diffusion of lipids may be characterized by the continuum models described above, which neglect the discreteness of the lipid matrix, which may only be valid for large membrane proteins.

Alternatively, a free area model based on the free volume theory (Cohen and Turnbull, 1959) was derived to calculate diffusion coefficients based on the microstructure of a two-dimensional system (Galla et al., 1979):

$$D = D(a^*) \exp\left(-\frac{\gamma a^*}{a_f}\right) \quad (4)$$

In this expression  $a^*$  is a critical free area available for a diffusor, below which no diffusion takes place,  $D(a^*)$  is the diffusion coefficient in a free area,  $a_f = a_f(T)$  is the average free area in the system, and  $\gamma$  is a geometric factor. In more general expressions an activation term,  $E_a/kT$ , is added to the argument of the exponential (Chung, 1966).

The decay of diffusion coefficients upon dehydrating a supported monolayer membrane could be linearized by performing an axis transformation in terms of a double logarithmic plot of the diffusion coefficient against the ratio of the partial water pressures,  $p_0/p$  (see, e.g., Fig. 3). In the following, a simple model shall be derived that explains this observation, taking into account a humidity-dependent activation energy for hopping events.

The quantity  $\ln(p_0/p)$  is proportional to the pressure difference,  $\Pi$ , (effective osmotic pressure) with respect to water saturation, according to:

$$\Pi = (kT/\nu) \ln(p_0/p) \quad (5)$$

where  $\nu$  is the volume of a water molecule and  $k$  is Boltzmann's constant. Equation 5 follows from the equality of the chemical potential differences  $\mu$  in the water film  $\mu = -\Pi \cdot \nu$  and in the gas phase  $\mu = kT \ln(p/p_0)$  with respect to a water bulk phase (Derjaguin et al., 1987).

A basic assumption of the model to be derived in the following is that diffusion can be regarded as an activated hopping process, which results in an Arrhenius-type diffusion behavior:

$$D = D_0 \cdot \exp(-E_a/kT) \quad (6)$$

Hopping thus takes place in a two-dimensional, triangular (Pink, 1983) lattice, with an activation energy,  $E_a$ , to perform a hopping step.

Furthermore, it is assumed that the diffusional activation energy is related to the adsorption energy (Clark, 1970; Adamson, 1990). For the derivation of our diffusion model, it is assumed that the humidity influence on the adsorption energy is dominated by humidity-dependent hydration forces between the monolayer and the underlying substrate. This assumption is based on the following argumentation.

The disjoining pressure  $\Pi(d)$  between planar, hydrophilic surfaces can be divided into three different contributions (Israelachvili and Wennerstroem, 1992).

$$\Pi(d) = \Pi_{dl}(d) + \Pi_{vw}(d) + \Pi_{hyd}(d) + \Pi(d)_{other} \quad (7)$$

In Eq. 7  $\Pi(d)$  is the total disjoining pressure, depending on the separation distance,  $d$ ,  $\Pi_{dl}(d)$  is an electrostatic double layer contribution,  $\Pi_{vw}(d)$  arises due to van der Waals interactions between the surfaces,  $\Pi_{hyd}(d)$  is a disjoining pressure due to hydration forces, and  $\Pi(d)_{other}$  represents additional contributions, such as steric repulsion or a disjoining pressure due to undulation forces. Numerous studies performed with lipid bilayer stacks have shown that in the case of zwitterionic lipids the hydration force dominates all other contributions for distance regimes between 0.5 and 30 Å (see Leikin et al., 1993; Rand and Parsegian, 1989, and references therein). Even in the case of charged lipids, at short separation distances (20–30 Å, depending on charge density), the hydration force dominates, whereas at greater distances exponentially decaying double layer forces constitute the main contribution to the membrane repulsion (Cowley et al., 1978). The transition between the two regimes is indicated by a change in the decay constant of the total disjoining pressure (Parsegian et al. 1991). In the present work zwitterionic lipids and in most cases a very weak polysaccharide polyelectrolyte was used. Moreover, in our diffusion experiments, no evidence for a transition between regimes of different interaction force decay constants was found.

To derive an appropriate model that focuses on the influence of hydration on lateral diffusion, all parameters which are, in a first approximation, independent of the relative humidity, are assumed to define the preexponential factor in Eq. 6. In particular, it is assumed that the free area available for diffusion is independent of  $RH$ , therefore the relevant parameters (Eq. 4) can be incorporated into  $D_0$ . The latter assumption will be rationalized further below. Thus  $D_0$  is the diffusion coefficient found for a particular substrate-supported monolayer in the fully hydrated state. The adsorption energy is dependent on  $RH$  and the hydration pressure contribution can be calculated by an integration of the disjoining pressure along the surface normal (Rand and Parsegian, 1989). A correlation between  $RH$  and the activation energy for diffusion has previously been assumed in Berman et al., 1997.

The lipid layer may be regarded as being partially fixed in a periodic lattice of potential wells (Oshanin et al., 1998;

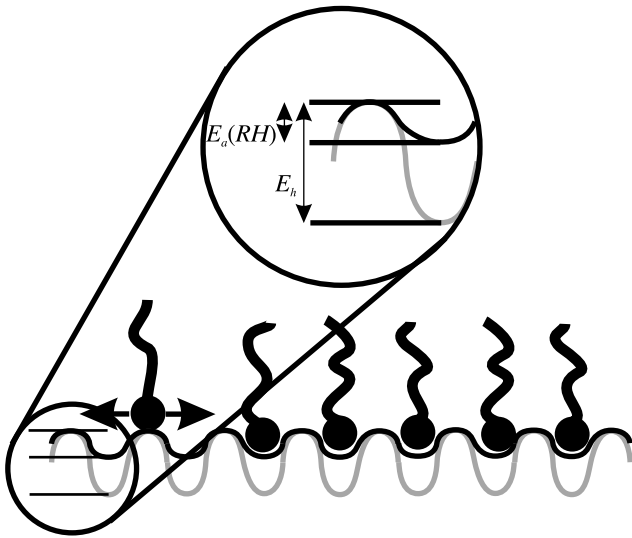


FIGURE 8 Lattice model for humidity-dependent activated diffusion in a substrate-supported lipid monolayer. Gray line: depth of potential wells ( $E_h$ ) in the completely dry state. Black line: depth of the potential wells ( $E_a(RH)$ ) at the relative humidity  $RH$ .

Auch et al., 2000), the depths of which are dependent on the state of hydration in the monolayer/substrate interface (Fig. 8). The depth of the wells is very deep concerning desorption to the gas phase, but allows for lateral jumps (Oshanin et al., 1998).

While the forces that contribute to the experimentally observed hydration force are to date poorly understood, simple empirical relations exist in most cases (Leikin et al., 1993). To calculate the activation energy change by alteration of  $RH$ , the empirical exponential relation between disjoining pressure,  $\Pi_{\text{hyd}}$ , and distance,  $d$ , (Eq. 8) between the surfaces is used, which holds for the swelling of lipid bilayer staples (Rand and Parsegian, 1989) and numerous other biological compounds (Leikin et al., 1993). In the present case, it is assumed that the same relation describes the disjoining pressure in the membrane/support interface (Rädler et al., 1995).

$$\Pi_{\text{hyd}} = \Pi_0 \exp(-d/\lambda_w) \quad (8)$$

$\Pi_0$  is an internal pressure, which is obtained by extrapolation to  $d = 0$ , and  $\lambda_w$  is a decay length. In the pressure range where Eq. 8 holds, i.e., in a distance regime between 0.5 and 3 nm, the disjoining pressure is equal to the osmotic pressure (Parsegian et al., 1979).

The combination of Eqs. 5 and 8 yields for the equilibrium distance:

$$d(p_0/p) = -\lambda_w \ln\left(\frac{\Pi_{\text{hyd}}}{\Pi_0}\right) = -\lambda_w \ln\left(\frac{kT}{\Pi_0 v} \ln\left(\frac{p_0}{p}\right)\right) \quad (9)$$

Equation 9 again is valid only in the distance regime between 0.5 and 3 nm, where the hydration force dominates

the surface forces. In the completely dry state, the hydration pressure contribution  $E_a$  to the activation energy corresponds to the energy  $E_h$  necessary to dehydrate a lipid headgroup, which can be approximated according to

$$E_h = a \int_{d=0}^{\infty} \Pi_{\text{hyd}} dd = \lambda_w a \Pi_0 \quad (10)$$

where  $a$  is the area of a lipid headgroup. In fact, Eq. 10 slightly underestimates the hydration energy, due to an upward deviation of  $\Pi_{\text{hyd}}$  at distances below 0.5 nm (Israelachvili and Wennerstrom, 1990). In a partially hydrated state,  $E_a$  is reduced (lower depth of potential wells) by the humidity-dependent disjoining pressure, i.e.,

$$\begin{aligned} E_a &= E_h - a \int_{d=0}^{d(p_0/p)} \Pi_{\text{hyd}} dd \\ &= a \cdot \Pi_0 \cdot \lambda_w \cdot \exp\left(-\frac{1}{\lambda_w} d(p_0/p)\right) \end{aligned} \quad (11)$$

Substitution for  $E_a$  in Eq. 6 yields:

$$\ln D = \ln D_0 - 1/(kT) \cdot a \cdot \Pi_0 \cdot \lambda_w \cdot \exp(-d(p_0/p)/\lambda_w) \quad (12)$$

and with Eq. 9 it follows:

$$\ln D = \ln D_0 - C \ln(p_0/p) \quad (13)$$

with

$$C = a \cdot \lambda_w / v \quad (14)$$

According to Eq. 13, a plot of  $\ln(D)$  versus  $\ln(p_0/p)$  should result in a straight line with the slope  $-C$  and an intercept of  $\ln(D_0)$ , which is consistent with the data (e.g., Fig. 3). In the following, the assumptions, limitations, and the information that can be drawn from the model shall be examined.

According to Eq. 14, a correlation between the slope,  $-C$ , obtained by humidity-dependent diffusion measurements and the decay parameter,  $\lambda_w$ , of the hydration force exists, which is the basic conclusion to be drawn from the model. To calculate  $\lambda_w$ , the following parameters were used. The volume of a water molecule is  $v = 30 \text{ \AA}^3$ , which may be obtained from the molarity of water (55 mol/l). Furthermore, the area  $a$  was approximated according to the area of a fully hydrated DMPC headgroup  $a = 60 \text{ \AA}^2$ , which corresponds both to a fully hydrated headgroup in a bilayer (Perera et al., 1996), and to the molecular area at the transfer pressure of the monolayer (Baumgart, 2001). By means of these parameters, from the slope  $C = -13.4$  obtained from Fig. 3 for diffusion measurements in a DMPC monolayer labeled with NBD-PE, a decay constant  $\lambda_w = 6.7 \text{ \AA}$  can be calculated. Experimentally obtained values (e.g., by the method of osmotic stress (Rand and Parsegian, 1989)) for



the decay constant of the hydration force (determined in bilayers) lie in the range of 0.8–6.4 Å (Rand and Parsegian, 1989; Marsh, 1989). The highest values are found for lysolipids. In the case of DMPC bilayer swelling, a value of 2.2 Å was obtained (Ionov and Angelova, 1996). The discrepancy is partially due to the different systems studied, here a solid-supported monolayer and there a multibilayer stack. Furthermore, the difference may be due to the apparent oversimplifications of the model. First, the actual cross-sectional area of the lipid headgroup in a partially dehydrated monolayer is smaller compared to the value measured by means of the film-balance in the completely hydrated state which, according to Eq. 14, will lead to a lower decay parameter. Second, in the derivation of Eq. 13 the swelling of the polymer cushion (Baumgart, 2001), which could lead to a reduction of lipid binding sites, was completely neglected. Third, the interparticle interactions within the lipid monolayer, which may vary upon changing  $RH$ , were neglected also.

From the linear fit to the data shown in the inset of Fig. 3, a diffusion coefficient  $D_0 = 6.4 \mu\text{m}^2/\text{s}$  (corresponding to complete hydration) was obtained, which is considerably smaller compared to diffusion coefficients measured at the air/water interface (in the case of, e.g., DLPC monolayers at a lateral pressure of 35 mN/m at room temperature, a value of  $D = 20 \mu\text{m}^2/\text{s}$  was found (Peters and Beck, 1983)). The smaller value in the present case indicates viscous friction in the lubrication layer between monolayer and polymer support (Evans and Sackmann, 1988).

Equation 13 is valid only for not too high disjoining pressures, due to the nonconvergence of Eq. 5 with respect to a zero relative humidity, contrary to Eq. 8, which converges for zero distance. This condition is fulfilled in the present experiments, since  $RH$  always was above 50%. In no case of the fluidity/humidity scans performed in the present work was a discontinuity (in terms of a deviation from linearity of the double logarithmic plot) observed. Furthermore, monolayers of DPhyPC, a lipid that does not show a first-order phase transition in bilayers down to a temperature of  $-120^\circ\text{C}$  were observed to exhibit the same linear relationship as compared to monolayers consisting of DMPC, a lipid that shows the main transition in bilayers at a temperature of  $23.8^\circ\text{C}$ . Additionally, a change in the lateral pressure of the supported monolayer did not lead to deviations from linearity in the axis-transformed plots. From these facts it can clearly be deduced that sharp first-order transitions induced by dehydration were not present in the hydrogel-supported monolayers examined in this work. As already mentioned, this observation is contrary to the case of multibilayer stacks. In the following paragraph, this difference shall be discussed and phase transitions of solid-supported monolayers will be examined in the light of observations to be found in the literature.

It has been pointed out by a number of authors that monolayers deposited onto a solid substrate by LB-transfer

can possess a higher lateral pressure on the support as compared to a floating monolayer on the trough subphase (Riegler and LeGrange, 1988; Riegler and Spratte, 1992; Spratte and Riegler, 1994; Sikes et al., 1996; Sikes and Schartz, 1997; Yaminsky et al., 1997). The solid-supported monolayer may even be in a different phase state. This phenomenon is known as substrate-mediated condensation and occurs in the meniscus region during transfer (Riegler and LeGrange, 1988). It is due to either the interaction between headgroups and the solid surface (e.g., Sikes et al., 1996), or to different pH values in the thin meniscus compared to the bulk water phase (e.g., Riegler and LeGrange, 1988). All of the above-cited works deal with phase transitions, which occur *during* the LB-transfer. Other groups reported morphological changes during storage, i.e., *after* the transfer. Chi et al. observed aging effects of polymer-supported stearic acid monolayers (Chi et al., 1993, 1994). It was assumed that water is transported together with the monolayer onto the solid substrate and that subsequent dehydration would increase the phase transition temperature of the monolayer, causing more molecules to be involved in a phase transition to a more condensed phase. In other works, phase transitions of polymer-supported, charged monolayers were observed by fluorescence microscopy and the transition temperatures were found to be increased with respect to monolayers at the air/water interface (Chi et al., 1992a,b) and further increased in case of glass-supported monolayers. Again, the change in the phase transition temperature was attributed to be influenced by changes in the hydration state of the polar headgroups, modulated by different supports (water, hydrophilic polymers, or glass) and ambient humidity. Fluorescence microscopy allows following phase transitions in amphiphile membranes, because the dye solubility is usually lower in condensed phases (Möhwald, 1990) (provided that the domains have a size above the resolution of the optical microscope). However, in the present work, in no case was the formation of domains upon dehydrating the monolayer found in fluorescence micrographs. Moreover, contrary to the works cited above, Shiku and Dunn (1998) found no evidence for phase transitions in solid-supported DPPC monolayers, deposited in the coexistence region, upon varying  $RH$ .

A first-order fluid/solid transition is necessarily accompanied by a lateral compression. As the surface area of the support is fixed, such a lateral compression would involve a partial dewetting of the monolayer. In this case, monolayer mobility would have to be analyzed in terms of percolation models (Saxton, 1982) and a percolation threshold would exist. Such a dewetting is, however, energetically unfavorable due to the high spreading power of lipid monolayers on substrates with high surface energies (Kühner et al., 1994). This is contrary to the case of lipid bilayer stacks, where the spreading parameter (for a bilayer spreading on top of another bilayer) in case of completely hydrated choline headgroups is even negative, as only a single bilayer spreads

on hydrated solid surfaces (Rädler et al., 1995). Therefore, the influence of relative humidity on the phase behavior of monolayers on high surface energy substrates on the one hand, and multibilayer stacks on the other hand, cannot be directly compared. It is likely that phase transitions in solid-supported monolayers cannot be described by a unique, effective lateral pressure caused by dehydration of lipid headgroups as in the case of multibilayer stacks (Parsegian et al., 1979). On the contrary, in case of a solid-supported monolayer, the special and complex monolayer/support interactions have to be taken into account, which includes electrostatic interactions and surface roughness effects. Clearly, further examinations are needed to analyze the transition orders and parameters, which influence humidity induced phase transitions in solid-supported monolayers.

With a higher lateral pressure, the slopes of the linear fits decrease (Fig. 4), which—according to Eq. 14—corresponds to a decrease in  $\lambda_w$ . While to the best of the author's knowledge no analysis concerning the lateral pressure dependence of the hydration force of solid-supported monolayers exists, generally, lipid bilayers in the gel phase show smaller decay constants compared to those in the fluid state (Israelachvili and Wennerstroem, 1992; Marsh, 1989). Whether the trend concerning the decay constants in Fig. 4 can be explained by a higher area fraction of solid condensed domains with increasing lateral pressure (see also Pink et al., 1995) can only be assumed, however.

In the derivation of Eq. 13 a crucial assumption was that the nature of the substrate plays a minor role concerning the lateral diffusion properties in monolayers at different relative humidities. While a direct and independent proof of the above-mentioned hypothesis is not feasible (monolayers always have to be supported by a substrate), it is possible to compare different substrates with respect to their influence on diffusion/humidity diagrams.

The comparison depicted in Fig. 5 strongly supports the hypothesis that the relationship expressed by Eq. 13 is independent from the nature of the actual substrate (as long as it is hydrophilic) and that Eq. 13 might therefore be assumed to be as generally applicable to local dynamics dependent on the state of hydration as the universal validity of the exponential distance dependence on the hydration force itself.

## CONCLUSIONS

Supported lipid monolayers were analyzed in terms of the lateral self-diffusion of lipid molecules as a function of relative humidity. Applying the Evans-Sackmann theory revealed that the reduced fluidity at decreasing values of *RH* could not be explained by assuming no-slip boundaries and viscous dissipation in a thin water film between monolayer and support. However, a universal response toward humidity changes was found for a variety of lipids in miscella-

neous conditions and for two different substrates. Plotting the logarithm of the measured diffusion coefficients against  $\ln(p_0/p)$ , a quantity proportional to the applied osmotic pressure, essentially yielded a straight line in all cases. This was explained by assuming a reduction of activation energies for diffusion by hydration, i.e., the reduction of effective osmotic pressure. A simple model was derived, a crucial assumption of which is an exponential decay of the disjoining pressure with distance from the surface of the monolayer support. From the model, a decay constant of the hydration force in the monolayer/support system was calculated and found to be higher compared to the case of multibilayer stacks, which was explained by apparent oversimplifications of the model and the absence of interleaflet interactions in solid-supported monolayers.

Furthermore, no indications were found for humidity-induced phase transitions in hydrogel-supported monolayers. This is also contrary to the case of multibilayer staples, where reducing the relative humidity exerts an effective lateral pressure leading to bilayer compression. The difference was explained by the high surface energy of the support, which prevents the monolayer from partial dewetting. Finally, it was qualitatively shown that fluidity enhancement in solid-supported lipid monolayers was not restricted to water—it was also found in the case of non-aqueous solvents. This is in accordance with the fact that “hydration” forces are no peculiar feature of water (structure effects) only—as was long believed and only recently shown to be erroneous (Israelachvili and Wennerstroem, 1990, 1992).

Many biological processes, such as vesicle fusion and recognition processes, are accompanied by dehydration/hydration cycles and it is reasonable to assume that the water activity significantly affects the kinetics of these processes in a manner outlined above. Several important aspects could not be covered by the present study. It would be particularly interesting to examine a broader range of different supports to clarify whether the universal relation found in the case of chitosan and agarose also holds for other supports. The influence of roughness effects could be another important aspect of diffusion in supported monolayers. Two improvements of the experimental setup are desired. A much more precise temperature control should allow for a refined analysis, especially in the high humidity regime; this should allow for the analysis of supports such as glass. Furthermore, the possibility to observe the monolayer directly (through a gas gap rather than through the support) would further widen the range of different (including nontransparent) substrates. Moreover, a determination of the hydration force itself, by measuring the membrane-substrate distance as a function of hydration, would further allow for a more precise data interpretation. While such measurements are complicated by the swelling of a hydrogel support normal to the surface, an advantageous experimental configuration could be a substrate-supported “foam

## Gas phase

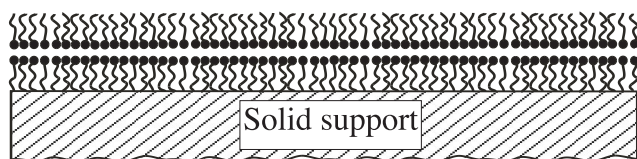


FIGURE 9 A solid-supported “foam film” as a possible experimental configuration for studying both lateral diffusion and the thickness of the interface between the two amphiphile leaflets.

film” as proposed in Fig. 9. The proximal monolayer would be transferred onto a hydrophobised substrate or chemically attached. In free-standing foam films, a correlation between the thickness of the water film and monolayer mobility has been found in a number of works (Lalchev et al., 1994, 1995). In that case, however, the thickness of the water layer was adjusted by the salt concentration, which regulates DLVO forces. The setup depicted in Fig. 9, however, would allow for a refined study of lateral diffusion in foam films with water layers of molecular thickness, and thickness measurements in parallel.

The authors thank Wolfgang Knoll for his generous support within the project and Diethelm Johannsmann for the donation of the apparatus for controlling relative humidities. Andreas Scheller is acknowledged for his help with the computer program, which controlled the humidity apparatus. Jürgen Worm kindly developed the program FRAP-fit, which enabled the analysis of diffusion raw data.

## REFERENCES

- Adamson, A. W. 1990. *Physical Chemistry of Surfaces*. Wiley, New York, Chichester, Brisbane, Toronto, Singapore.
- Almeida, P. F. F., and W. L. C. Vaz. 1995. Lateral diffusion in membranes. In *Handbook of Biological Physics*. A. J. Hoff, editor. Elsevier, Amsterdam.
- Auch, M., B. Fischer, and H. Möhwald. 2000. Lateral lipid diffusion in phospholipid monolayers coupled to polyelectrolyte films. *Colloids Surfaces A: Physicochem. Eng. Aspects*. 164:39–45.
- Axelrod, D., D. E. Koppel, J. Schlessinger, E. Elson, and W. W. Webb. 1976. Mobility measurement by analysis of fluorescence photobleaching recovery kinetics. *Biophys. J.* 16:1055–1069.
- Balcom, B. J., and N. O. Petersen. 1993. Lateral diffusion in model membranes is independent of the size of the hydrophobic region of molecules. *Biophys. J.* 65:630–637.
- Baumgart, T. 2001. *Preparation and Physicochemical Characterisation of Planar Supported Lipid Model Membrane Systems*. Ph.D. thesis, Johannes Gutenberg Universität, Mainz, Germany.
- Berman, A. D., S. D. Cameron, and J. N. Israelachvili. 1997. Mobility of surfactants in and between adsorbed monolayers. *J. Phys. Chem. B*. 101:5692–5697.
- Blair, H. S., J. Huthrie, T.-K. Law, and P. Turkington. 1987. Chitosan and modified chitosan membranes. I. Preparation and characterization. *J. Appl. Polym. Sci.* 33:641–656.
- Bolze, J., M. Takahasi, J. Mizuki, T. Baumgart, and W. Knoll. 2002. X-ray reflectivity and diffraction studies on lipid and lipopolymer Langmuir–Blodgett films under controlled humidity. *J. Am. Chem. Soc.* In press.
- Chattopadhyay, A. 1990. Chemistry and biology of *N*-(7-nitrobenz-2-oxa-1,3-diazol-4-yl)-labeled lipids: fluorescent probes of biological and model membranes. *Chem. Phys. Lipids*. 53:1–15.
- Chattopadhyay, A., and S. Mukherjee. 1999. Depth-dependent solvent relaxation in membranes: wavelength-selective fluorescence as a membrane dipstick. *Langmuir*. 15:2142–2148.
- Chen, Y. L. E., M. L. Gee, C. A. Holm, J. N. Israelachvili, and P. M. McGuiggan. 1989. Effects of humidity on the structure and adhesion of amphiphilic monolayers on mica. *J. Phys. Chem.* 93:7057–7059.
- Chen, Y.-L., and J. Israelachvili. 1992. Effects of ambient conditions on adsorbed surfactant and polymer monolayers. *J. Phys. Chem.* 96:7752–7760.
- Chi, L. F., M. Anders, H. Fuchs, R. R. Johnston, and H. Ringsdorf. 1993. Domain structures in Langmuir–Blodgett films investigated by atomic force microscopy. *Science*. 259:213–216.
- Chi, L. F., H. Fuchs, R. R. Johnston, and H. Ringsdorf. 1994. Investigation of phase-separated Langmuir–Blodgett films by atomic force microscopy. *Thin Solid Films*. 242:151–156.
- Chi, L. F., R. R. Johnston, and H. Ringsdorf. 1992a. Mobile supported monolayers of ionic amphiphiles: variation of domain morphology via preadsorbed polyelectrolytes. *Langmuir*. 8:1360–1365.
- Chi, L. F., R. R. Johnston, H. Ringsdorf, N. Kimizuka, and T. Kunitake. 1992b. Polymeric gegenions induced variability and mobility of amphiphilic supramolecular structures on solid substrates. *Thin Solid Films*. 210:111–113.
- Chung, H. S. 1966. On the Macedo-Litovitz hybrid equation for liquid viscosity. *J. Chem. Phys.* 44:1362–1364.
- Clark, A. 1970. *The Theory of Adsorption and Catalysis*. Academic Press, New York, London.
- Clegg, R. M., and W. L. C. Vaz. 1985. Translational diffusion of proteins and lipids in artificial lipid bilayer membranes. A comparison of experiment with theory. In *Progress in Protein Lipid Interactions*, Vol. 1. A. Watts and J. J. De Pont, editors. Elsevier/North Holland, Amsterdam. 173–229.
- Cohen, M. H., and D. Turnbull. 1959. Molecular transport in liquids and glasses. *J. Chem. Phys.* 31:1164–1169.
- Cowley, A. C., N. L. Fuller, R. P. Rand, and V. A. Parsegian. 1978. Measurement of repulsive forces between charged phospholipid bilayers. *Biochemistry*. 17:3163–3168.
- Derjaguin, B. V., N. V. Churaev, and V. M. Muller. 1987. *Surface Forces*. Plenum Publishing Corporation, New York, London.
- Dietrich, C., and R. Tampe. 1995. Charge determination of membrane molecules in polymer-supported lipid layers. *Biochim. Biophys. Acta*. 1238:183–191.
- Evans, E., and E. Sackmann. 1988. Translational and rotational drag coefficients for a disk moving in a liquid membrane associated with a rigid substrate. *J. Fluid Mech.* 194:553–561.
- Galla, H. J., W. Hartmann, U. Theilen, and E. Sackmann. 1979. On two-dimensional passive random walk in lipid bilayers and fluid pathways in biomembranes. *J. Membr. Biol.* 48:215–236.
- Galle, J., and F. Volke. 1995. Computer simulation of the temperature- and hydration-dependent lateral diffusion of phosphatidylcholine in lipid bilayers. *Biophys. Chem.* 54:109–117.
- Györfvay, E., B. Wetzter, U. B. Sleytr, A. Sinner, A. Offenhäusser, and W. Knoll. 1999. Lateral diffusion of lipids in silane-, dextran-, and S-layer-supported mono and bilayers. *Langmuir*. 15:1337–1347.
- Ho, C., and C. D. Stubbs. 1997. Effect of *n*-alkanols on lipid bilayer hydration. *Biochemistry*. 36:10630–10637.
- Ionov, R., and A. Angelova. 1996. Swelling of bilayer lipid membranes. *Thin Solid Films*. 284/285:809–812.
- Israelachvili, J. N., and H. Wennerstroem. 1990. Hydration of steric forces between amphiphilic surfaces. *Langmuir*. 6:873–876.
- Israelachvili, J. N., and H. Wennerstroem. 1992. Entropic forces between amphiphilic surfaces in liquids. *J. Phys. Chem.* 96:520–531.

- Kühner, M., R. Tampe, and E. Sackmann. 1994. Lipid mono and bilayer supported on polymer films: composite polymer-lipid films on solid substrates. *Biophys. J.* 67:217–226.
- Lalchev, Z., R. Todorov, H. Ishida, and H. Nakazawa. 1995. Lateral mobility of phospholipid molecules in thin liquid films. *Eur. Biophys. J.* 23:433–438.
- Lalchev, Z. I., P. J. Wilde, and D. C. Clark. 1994. Surface diffusion in phospholipid foam films. *J. Colloid Interface Sci.* 167:80–86.
- Leikin, S., A. Parsegian, and D. C. Rau. 1993. Hydration forces. *Annu. Rev. Phys. Chem.* 44:369–395.
- Lindsey, H., N. Peterson, and S. Chan. 1979. Physicochemical characterization of 1,2-diphytanoyl-sn-glycero-3-phosphatidylcholine in model membrane systems. *Biochim. Biophys. Acta.* 555:147–167.
- Marsh, D. 1989. Water adsorption isotherms and hydration forces for lysolipids and diacyl phospholipids. *Biophys. J.* 55:1093–1100.
- McCown, J. T., E. Evans, S. Diehl, and H. C. Wiles. 1981. Degree of hydration and lateral diffusion in phospholipid multibilayers. *Biochemistry.* 20:3134–3138.
- McIntosh, T. J., A. D. Magid, and S. A. Simon. 1989. Range of the solvation pressure between lipid membranes: dependence on the packing density of solvent molecules. *Biochemistry.* 28:7904–7912.
- Merkel, R., E. Sackmann, and E. Evans. 1989. Molecular friction and epitactic coupling between monolayers and supported bilayers. *J. Phys. France.* 50:1535–1555.
- Möhwald, H. 1990. Phospholipid and phospholipid-protein monolayers at the air/water interface. *Annu. Rev. Phys. Chem.* 41:441–476.
- Neuman, R. D., S. Park, and P. Shah. 1994. Lateral diffusion of surfactant monolayer molecules confined between two solid surfaces. *J. Phys. Chem.* 98:12474–12477.
- Oshanin, G., J. D. De Coninck, A. M. Cazabat, and M. Moreau. 1998. Microscopic model for spreading of a two-dimensional monolayer. *J. Mol. Liquids.* 76:195–219.
- Parsegian, V. A., N. Fuller, and R. P. Rand. 1979. Measured work of deformation and repulsion of lecithin bilayers. *Proc. Natl. Acad. Sci. USA.* 76:2750–2754.
- Parsegian, V. A., R. P. Rand, and N. L. Fuller. 1991. Direct osmotic stress measurements of hydration and electrostatic double-layer forces between bilayers of double-chained ammonium acetate surfactants. *J. Phys. Chem.* 95:4777–4782.
- Perera, L., U. Essmann, and M. L. Berkowitz. 1996. Role of water in the hydration force acting between lipid bilayers. *Langmuir.* 12:2625–2629.
- Peters, R., and K. Beck. 1983. Translational diffusion in phospholipid monolayers measured by fluorescence microphotolysis. *Proc. Natl. Acad. Sci. USA.* 80:7183–7187.
- Pink, D. A. 1983. Theoretical studies of phospholipid bilayers and monolayers. Perturbing probes, monolayer phase transitions, and computer simulations of lipid-protein bilayers. *Can. J. Biochem. Cell Biol.* 62:760–777.
- Pink, D., M. Kühner, B. Quinn, E. Sackmann, and H. Pham. 1995. Evidence for domains in deposited lipid bilayers. *Langmuir.* 11:2696–2704.
- Rädler, J., H. Strey, and E. Sackmann. 1995. Phenomenology and kinetics of lipid bilayer spreading on hydrophilic surfaces. *Langmuir.* 11:4539–4548.
- Rand, R. P., and V. A. Parsegian. 1989. Hydration forces between phospholipid bilayers. *Biochim. Biophys. Acta.* 988:351–376.
- Riegler, J. E., and J. D. LeGrange. 1988. Observation of a monolayer phase transition on the meniscus in a Langmuir-Blodgett transfer configuration. *Phys. Rev. Lett.* 61:2492–2495.
- Riegler, H., and K. Spratte. 1992. Structural changes in lipid monolayers during the Langmuir-Blodgett transfer due to substrate/monolayer interactions. *Thin Solid Films.* 210/211:9–12.
- Sackmann, E. 1996. Supported membranes: scientific and practical applications. *Science.* 271:43–48.
- Sackmann, E., and M. Tanaka. 2000. Supported membranes on soft polymer cushions: fabrication, characterization and applications. *Tibtech.* 18:58–64.
- Saffman, P. G. 1975. Brownian motion in thin sheets of viscous fluid. *J. Fluid Mech.* 73:593–602.
- Saxton, M. 1982. Lateral diffusion in an archipelago: effects of impermeable patches on diffusion in a cell membrane. *Biophys. J.* 39:165–173.
- Shiku, H., and R. C. Dunn. 1998. Direct observation of DPPC phase domain motion on mica surfaces under conditions of high relative humidity. *J. Phys. Chem. B.* 102:3791–3797.
- Sikes, H. D., and D. K. Schartz. 1997. A temperature-dependent two-dimensional condensation transition during Langmuir-Blodgett deposition. *Langmuir.* 13:4704–4709.
- Sikes, H. D., J. T. Woodward, and D. K. Schartz. 1996. Pattern formation in a substrate-induced phase transition during Langmuir-Blodgett transfer. *J. Phys. Chem.* 100:9093–9097.
- Sirota, E. B., G. S. Smith, C. R. Safinya, R. J. Plano, and N. A. Clark. 1988. X-ray-scattering studies of aligned, stacked surfactant membranes. *Science.* 242:1406–1409.
- Spratte, K., and H. Riegler. 1994. Steady state morphology and composition of mixed monomolecular films (Langmuir monolayers) at the air/water interface in the vicinity of the three-phase line: model calculations and experiments. *Langmuir.* 10:3161–3173.
- Vanderveen, R. J., and G. T. Barnes. 1985. Water permeation through Langmuir-Blodgett monolayers. *Thin Solid Films.* 134:227–236.
- Wolff, O. 1998. Bestimmung des viskoelastischen Verhaltens dünner und ultradünner Polymerfilme mit Hilfe von Schwingquarzen. Ph.D. thesis. Ruprecht-Karls-Universität, Heidelberg.
- Yaminsky, V., T. Nylander, and B. Ninham. 1997. Thermodynamics of transfer of amphiphiles between the liquid-air interface and a solid surface: wetting tension study of Langmuir-Blodgett films. *Langmuir.* 13:1746–1757.